JOURNAL OF TECHNIQUES

Journal homepage: http://journal.mtu.edu.iq

RESEARCH ARTICLE - ENGINEERING

Design and Implementation of a Healthcare Monitoring System Based on LoRa

Hayder Fadhil Jawad[1], Ali Al-Askery[1*], Adnan Hussein Ali[2]

[1]Electrical Engineering Technical College, Middle Technical University, Baghdad, Iraq.

[2] Institute of Technology / Baghdad, Middle Technical University, Baghdad, Iraq.

[*] Corresponding author E-mail: a.alaskery@mtu.edu.iq

Article Info.

Article history:

Received
30 July 2022

Accepted
18 August 2022

Publishing
31 December 2022

Abstract

For humans to survive, scientific and technological advancements must be able to contribute to the solution of human medical issues. The design and implementation of a monitoring system for the measurement of blood oxygen saturation, heart rate, and body temperature have been combined into one tool in this study. The measurement results are shown both on the measuring instrument's OLED display and a remote monitoring system's LCD display. This instrument uses ESP32 as a Microcontroller and LoRa as a wireless communication technique. The MLX90614 sensor is used to detect body temperature, while the MAX30100 sensor is used to monitor blood oxygen saturation and heart rate. Testing Measurements are calibrated using instruments that meet industrial standards (Wincom infrared thermometer and GE patient monitor) used in the hospital. When compared to industry-standard instruments, the tool's accuracy is 98.18% for measurements of blood oxygen saturation, 96.54 % for measurements of heart rate, and 98.78 % for measurements of body temperature. The instrument's total accuracy, calculated as the average of all three factors, was 97.63 %. If the abnormalities in the recorded parameters are detected, then an alert will be triggered (buzzer and blinking LED). this instrument can help the patients to check their health status and provide remote monitoring of health providers.

Publisher : Middle Technical University

Keywords: LoRa; HealthCare Station; MAX30100; MLX90614.

1. Introduction

The healthcare monitoring system is undergoing a metamorphosis that makes it feasible to monitor residents continuously even when they are not hospitalized. Healthcare surveillance is an increasingly common practice. The modern healthcare sector strives to offer better healthcare in an affordable and patient-friendly manner to individuals all over the world. The development of intelligent systems that continually monitor human activity has become possible because of advancements in sensor technologies, embedded systems, wireless communication technologies, nanotechnologies, and downsizing. Wearable sensors monitor physiological indicators combined with other symptoms to identify abnormal and/or unexpected events. As a result, assistance may be given when it's needed[1]. When it comes to patient monitoring, the medical industry now confronts two fundamental issues. The patient is confined to a bed and connected to huge machinery in the first instance, and there is a healthcare practitioner there in addition to the patient in the second. With the development of technology, it is now feasible to create a low-cost, at-home healthcare monitoring system that captures, visualizes and sends bodily signals to any other place[2]. As they become more comfortable and unobtrusive, wearable sensors are suitable for monitoring someone's health or wellness without interfering with their normal activities. By attaching the sensors to various body parts, the sensors can track a variety of physiological signals and data as well as a person's activity and mobility. Low-cost, unobtrusive, and long-term health is made possible by the development of low-power, small wearables (sensors, actuators, antennas, and smart textiles), affordable computation, and storage devices, as well as current communication technologies[3]. Heart rate, blood pressure, respiratory rate, blood oxygen saturation, and body temperature are the top five conventional vital signs that should be checked. The broad consensus is that these five signals are necessary to assess human health, and they should be continuously monitored, particularly in patients[4]. SpO2 is a crucial critical measure that is used to identify hypoxemia. SpO2 readings between 95 and 100% are considered optimal, When the SpO2 falls below 93 %, it is believed from a medical patient's point of view that immediate compensatory measures must be taken[5]. Using photoplethysmography (PPG) technology and pulse oximetry principles, it is simple to measure blood oxygen saturation (SpO2), a crucial metric that is exceedingly important. When monitored with two wavelengths (often 660 nm and 950 nm), the (PPG) technique permits the capture of blood vessel variation waveform, and it is feasible to determine blood oxygen saturation. This is because when hemoglobin binds to oxygen, the absorbance spectrum of hemoglobin changes. The quantity of oxygen transported by blood cells may be calculated using the oximetry principles (normally: 95–100%). When a patient is anemic, measuring blood oxygen saturation might be problematic[6]. PPG comes in two varieties: transmittance and reflectance. The light source and light detector are positioned on opposite sides of the tissue in transmittance (PPG). As a result, the tissue must be penetrated by the produced light before the detector may detect a change in the tissue. Consequently, this kind of PPG is only appropriate for usage in small-volume organs like (the ear lobe and fingers). Instead, the light source, the detector, and the reflectance type (PPG) are all positioned on the same side of the tissue. As a result, the light is emitted from the source into the tissue, and the detector then detects changes in the reflected light. As a result, this kind may be applied to any portion of the body[7].

Nomenclature

LCD Liquid Crystal Display	RTD Resistance Temperature Detectors
OLED Organic Light-Emitting Diode	I2C Inter-Integrated Circuit
LED Light-Emitting Diode	SCL Serial Clock
PPG Photoplethysmography	SDA Serial Data
ECG Electrocardiogram	BM Benchmark
BCG Ballistocardiogram	MAE Mean Absolute Error
CT Core Temperature	RMSE Root Mean Square Error
MAPE Mean Absolute Percentage Error	

Another physiological metric that wireless patient monitoring devices frequently employ is heart rate. It enables a diagnosis of the patient's state, fast recording of cardiac arrhythmias, and simple classification of alterations as normal or pathological. It was common practice to use this measure to deliver crucial data about cardiovascular function. Adult males typically have a resting heart rate of approximately 70 bpm while adult females typically have a resting heart rate of about 75 bpm[8]. Standard vital signs like heart rate are now often measured in both medical settings and physical fitness/sports. By detecting variations in the cardiac cycle, the monitoring of this signal reveals information about the physiologic condition. This vital sign is easily derived from photoplethysmography (PPG) or ECG (R-peak) data. These two physiological signals come from two separate physiological causes and include different morphologic information in their waveforms, yet they both contain information on heart rate. In comparison to the heart rate deduced from the electrocardiogram (ECG) and other methods, such as utilizing inertial sensors or scales, known as ballistocardiogram (BCG), there are additional ways to assess heart rate (PPG)[9]. However, body temperature may also be used as a general indicator of health. The range of the normal human body temperature is 36.1 to 37.2 degrees Celsius[10], depending on the activity level and location of the measurement. When a person becomes overheated, the blood vessels in their skin dilate to transfer the extra heat to their skin's surface. The person starts to perspire as a result. The perspiration then dries up, which aids in cooling the person's body. To conserve body heat, a person's blood vessels constrict when they are too cold, reducing blood flow to the skin. As a result, he or she begins to shiver, which is an uncontrollable, rapid contraction of the muscles[11]. Core temperature (CT) and skin temperature are the two components of body temperature. Since the body's thermoregulation systems control core temperature, skin temperature can vary across a larger range of temperatures than core temperature. Blood flow has an impact on skin temperature and is linked to both metabolic rate and heart rate. This body's internal thermostat is significantly influenced by external variables including air flow, temperature, and humidity. It is still difficult to measure (CT) using non-invasive techniques like skin temperature and heart rate collection. It is challenging to have a direct association between these variables that just rely on the human physiologic thermoregulation systems. This is mostly due to the extrinsic influences that might impact physiological indicators[12, 13]. Temperature can be measured by using different types of sensors. These sensors come in different forms such as thermocouples, thermistors, resistance temperature detectors (RTD), and integrated circuit (IC) sensors [14]. Happy Hypoxia, a condition where the body's oxygen saturation declines and can lead to shortness of breath in Covid-19 patients, is one of the symptoms of the disease. The amount of oxygen in the blood, also known as blood oxygen saturation, is a crucial physiological indicator for the respiratory and circulatory systems. When COVID-19 symptoms manifest, the patient's body temperature rises to greater than 38°C. To detect early lung damage in patients with Covid-19 and stop it from progressing, a monitoring device for the patient's oxygen saturation, heart rate, and body temperature is required[15]. The MAX30100, MAX30102, and MAX30105 sensors have been employed in several investigations as heart rate and oxygen saturation sensors. These sensors operate on the reflectance principle, where the light source and detector are located on the same side, allowing measurements to be made on different body sections[11, 15]. Temperature sensors must be included as well so that the equipment may be used to identify early signs of Covid-19 patients. The MLX90614 sensor was chosen as a non-contact body temperature sensor to prevent Covid-19 transmission. Much research has employed DS18B20 and LM35 sensors as temperature sensors[15–17]. A measuring device based on Lora's contact technology has been created for heart rate, oxygen saturation, and body temperature based on the above-mentioned biomarkers. To measure heart rate and oxygen saturation, the MAX30100 sensor was used. To prevent the spread of Covid-19 among patients and monitor the patient's temperature, the MLX90614 sensor was selected as the non-contact body temperature sensor. With LoRa, the measurement data is sent to a monitoring station, where the results are displayed on the LCD screen. With a warning system to alert the patient if their vital signs exceed the normal limit.

2. Methodology

2.1. Components of the instrument

The hardware circuit design and the components utilized in the suggested system will be displayed in this part. Additionally, the connection and programming procedures will be described together with the design that was utilized for the instrument. The parts of the planned healthcare station system will be displayed in this subsection all sensors mentioned in this subsection will be attached to Heltec WIFI LoRa 32 (V2) board for sending their data to the monitoring station through LoRa.

2.1.1. Body Temperature Sensor (MLX90614)

Body temperature is one of the key factors in health assessment because it reflects the patient's well-being. A patient's life may be in danger due to both a low body temperature and a high body temperature. In addition to these dangers, a non-life-threatening temperature increase can aid medical professionals in diagnosing illnesses. For these reasons and more, The MLX90614 Infrared Thermometer Sensor shown in Fig. 1A was used to read the temperature of the patient's body according to its high accuracy rate, short response time, small size, and low power consumption. The MLX90614 sensor was chosen as a non-contact body temperature sensor and therefore can use to avoid Covid-19 transmission.

Factory calibrated in a wide temperature range: -40 to +125°C for sensor temperature, High accuracy of +/- 0.5°C over a wide temperature range, Customizable PWM output for continuous reading. it can be used with Arduino or any microcontroller that can communicate with it through its (I2C) interface, the Inter-Integrated Circuit (I2C) Protocol is a protocol intended to allow multiple "peripheral" digital integrated circuits ("chips") to communicate with one or more "controller" chips. this sensor has four pins (VCC, GND, SCL, and SDA) the VCC pin is connected to 3.3v and the GND pin to the ground, the SCL pin to the SCL, and the SDA pin to the SDA of the microcontroller are shown in

Fig. 1B. The IR sensor consists of serially connected thermo-couples with cold junctions placed at thick chip substrate and hot junctions, placed over a thin membrane.

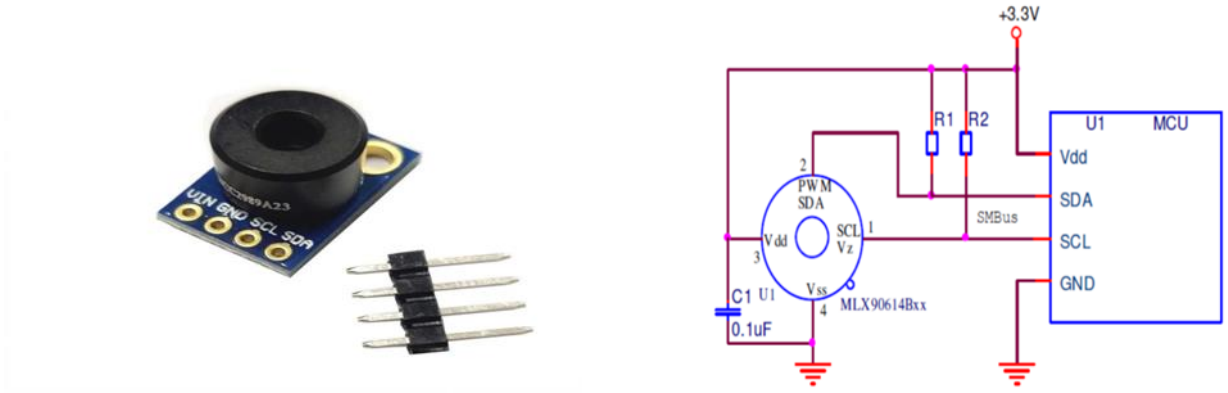

A B

Fig. 1. The temperature sensor (a) MLX90614 BCC and (b) connection to the microcontroller

2.1.2. Heart rate and oxygen saturation sensor (MAX30100)

MAX30100 is an integrated pulse oximetry that shows blood oxygen saturation level and heart beats per minute (bpm). It combines two LEDs (infrared and red), a photodetector, and optimized optics. Also, it has low-noise analogue signal processing to detect heart rate and pulse oximetry by using ADC 14-bit resolution. MAX30100 operates from 1.8V and 3.3V power supplies and can be powered down or sleep through software with a negligible standby current, permitting the power supply to remain connected at all times. it can be used with Arduino or any microcontroller that can communicate with it through its (I2C) interface. These and other specifications are demonstrated in Appendix B. MAX30100 was used in this study to read the pulse oximeter and heart rate to monitor the patients, and send the vital signs to the microcontroller to send data of vital signs to the monitoring station over LoRa and make decisions if the vital signs were abnormal. Also, these vital signs are displayed on the OLED screen. The principle of the sensor, how it works, and the operation that was used inside the sensors is illustrated in Fig. 2A, and the sensor is shown in Figure 2B. Equation (1) shows the pulse oximeter calculation, and Equation (2) calculates the frequencies that were given the heart rate in the second. Then, Equation (3) demonstrates the heart rate in minutes[18].

$$SpO2 = 10.0002R^3 + 26.817R + 98.29 \quad (1)$$

$$Frequency = 10^6/(BPMT\_T\_COUNT \times 10) \quad (2)$$

$$Heart\ rate = Frquency \times 60 \quad (3)$$

Where *R* is the ratio between two LEDs red and infrared, and *(BPMT_T_COUNT)* is the total count of the tick.

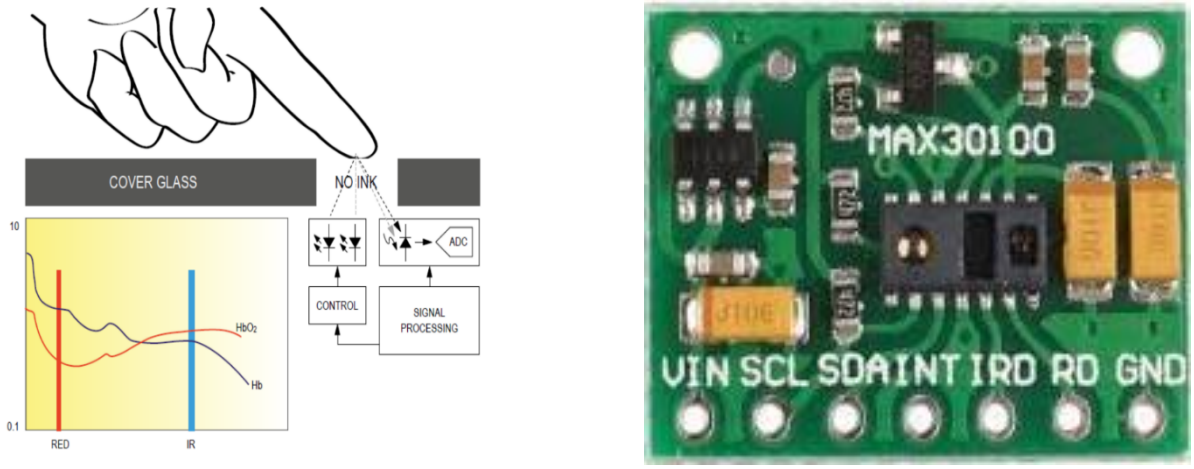

(A) (B)

Fig. 2. MAX30100 sensors (a) principal work of the sensors and (b) MAX30100 sensor

2.1.3. Heltec WIFI LoRa 32 (V2)

Heltec WIFI LoRa 32 (V2) is a classic IoT dev-board designed & produced by Heltec Automation, it's a highly integrated product based on ESP32 + SX127x, it has Wi-Fi, BLE, LoRa functions, also Li-Po battery management system, 0.96″ OLED are also included as shown in Fig. 3. It's the best choice for smart cities, smart farms, smart homes, and IoT makers. a Wi-Fi module made by the Chinese company Heltec Automation[19]. This module works on 3.3V and 5V with a maximum current consumption of 130mA at 20dB LoRa output. it has WIFI, BLE, and LoRa functions, it gives the ability to connect the microcontroller to the internet using IEEE 802.11 b/g/n Wi-Fi protocols. Also, the ability to connect the microcontroller to a mobile phone throw the BLE and LoRa which is used in our system. another advantage to using the Heltec WIFI LoRa 32 (V2) (V2) is that 0.96″ OLED is also included on the same board so there is no need to add an external display to the system

which in turn reduce the consumption of power. the microcontroller used in our system is ESP32 which is one of the main IoT learning tools. This offers a full Linux system on a small platform at a very low price. ESP32 connects device sensors and actuators through GPIO pins. ESP32 and IoT merge to be new technology for creativity in the healthcare system. ESP32 is designed extremely with integrated antenna switches, control amplification, low-noise amplifiers, and filters as well as power management modules. OLED is an advanced electronic piece as it is better than liquid crystal display (LCD) screens. The OLED works without a backlight because the OLED emits visible light. Thus, it can display deeper black levels, and it is thinner, lighter, and has a high resolution compared with LCD screens. In low surrounding light conditions (e.g., a darkroom), an OLED screen can achieve a higher disparity ratio than an LCD screen. It has low power consumption, doesn't reach 10mA, and has a high resolution at 128 × 64 pixels Thus; it is used to demonstrate vital signs (heart rate, Spo2, and temperature). In the proposed system the Heltec WIFI LoRa 32 (V2) was used as a wireless network interface which was responsible for making the connection between the ESP32 microcontroller and the remote monitoring station to send the data in real-time. Transmission distance (measured open area communication distance 2.8Km)[20].

.

Fig. 3. Heltec WIFI LoRa 32 (V2)

2.2. Circuit Design of Healthcare Station

The equipment required to be tiny and comfortable to wear without restricting the patient's movement to provide higher well-being while being worn, therefore the size was compact by using single-side PCB board with dimensions 5cm*7cm., as established in Fig. 4. The diagram of this circuit is shown in Fig. 5. The circuit was designed by the fritzing software. All the contents of the circuit were placed inside the plastic box with dimensions 6x6x4cmThis circuit is made up of several electronic components that have been crammed into a single electrical circuit and positioned on one side of the circuit to make it smaller. The soldering iron assisted to mount the pieces.

In addition, the charging module has been attached to this circuit which consists of a rechargeable flat lithium battery with 3.7v and 1200mah and a Lithium battery Charger board 5v 1A 18650 TP4056 as shown in Figs. 6 A and B. These and other components used in this proposed circuit are illustrated in Table 1. This circuit is portable, lightweight, and ideal for wrist wear as seen in Fig. 7. Heltec WIFI LoRa 32 (V2) board was connected to a Pc and programmed by the Arduino programming platform. by selecting the board type (Heltec WIFI LoRa 32 (V2) The bootloader was burned on the microcontroller to activate it and prepare it for use. The healthcare station measuring was contrasted with the standard medical equipment utilized at the hospital (Wincom infrared thermometer and GE patient monitor)[21], shown in Figures 8 A and B.

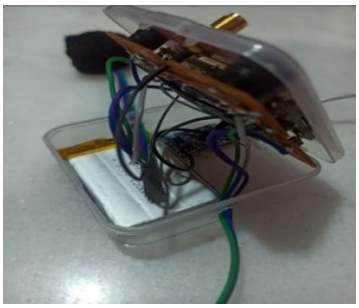

Fig. 4. PCB board with components

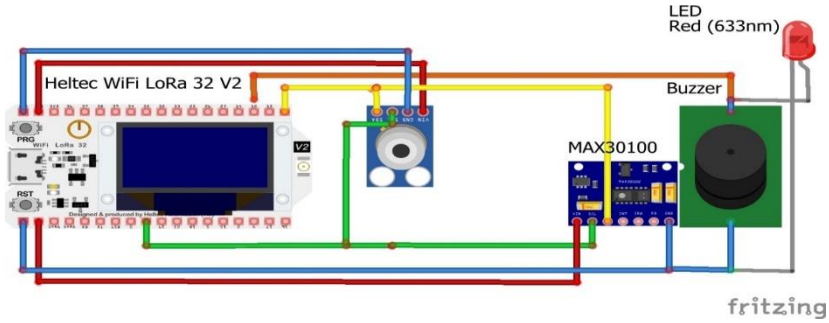

Fig. 5. The diagram of the healthcare station

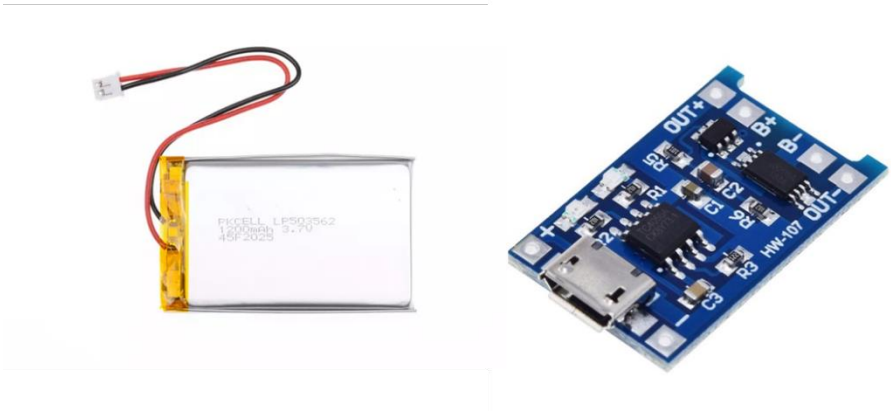

(A) (B)

Fig. 6. Charging module(a) rechargeable flat lithium battery and (b) Charger board TP4056

Fig. 7. Healthcare station during data measuring

(A) (B)

Fig. 8. Infrared thermometer(A) and patient monitor(B) Benchmark device

Table 1. The components of the Healthcare Station

No.	Components used	Quantity
1.	Heltec WIFI LoRa 32 (V2)	1
2.	Body Temperature Sensor (MLX90614)	1

3.	Heart rate and oxygen saturation sensor (MAX30100)	1
4.	Buzzer	1
5.	RED LED	1
6.	PCB Board	1
7.	Rechargeable flat lithium battery1200mah	1
8.	Charger board TP4056	1
9.	Switch	1
10.	Antenna (3dB)	1

2.3. Validation between the Proposed Healthcare Station and Benchmark device

The following readings from the instrument were collected during tests of measurements to ensure that the intended system worked correctly. This was dependent on two medical sensors: the Spo2 and also the MLX90614 to detect body temperature and the MAX30100 sensor to calculate the heart rate. Additionally, to deliver these values to the monitoring station, these readings were shown on an OLED panel. The tests were carried out in Iraq's Imam Al-Sadiq Hospital's intensive care unit, managed by the Babel Health Directorate. 30 participants, both male and female, ranging in age from 14 to 80, helped carry out the study. Over 14 days, the volunteers' measurements were taken. For each patient, the data were compared to benchmarks (BM), whose readings were acquired manually at the same time as the proposed device. To show that the proposed system is legitimate, the two special readings from the proposed device and the BM were then compared. Some experiments were done on the patients which are shown in Figs. 9 and 10 for the volunteers.

Fig. 9. The volunteers during measurements

Fig. 10. The volunteers during measurements

3. Results and Discussion

The results of the proposed healthcare station will be presented and discussed. These results are summarized into three categories: the validation of the measurement between both the healthcare station and the Benchmark device (BM), power consumption calculations, and the comparison between the proposed healthcare station and related works. In the validation of the measurement, the statistical analysis (i.e., error test and Pearson correlation coefficient) and the accuracy of the system of the proposed healthcare station compared to the BM will be presented,

clarified, and discussed. The power consumption calculations will present how much the healthcare station consumes electrical currents. and battery life.

3.1. Healthcare station measurement validity

To determine how accurate the system is, a statistical study between both the healthcare station and the Benchmark device (BM) was performed in this part. 35 samples were taken using a healthcare station, 35 of each for temperature, heart rate, and SpO2, as was demonstrated in the previous chapter. Additionally, a Benchmark device (BM) was used to obtain the same number. Figs. 11 (A, B, and C) which contrast the temperatures, heart rates, and oxygen saturation of the healthcare station and BM, respectively, reveal little difference between the two sets of findings. The next statistical studies, including the error test and Pearson correlation coefficient, will reveal whether or not these discrepancies are tolerable.

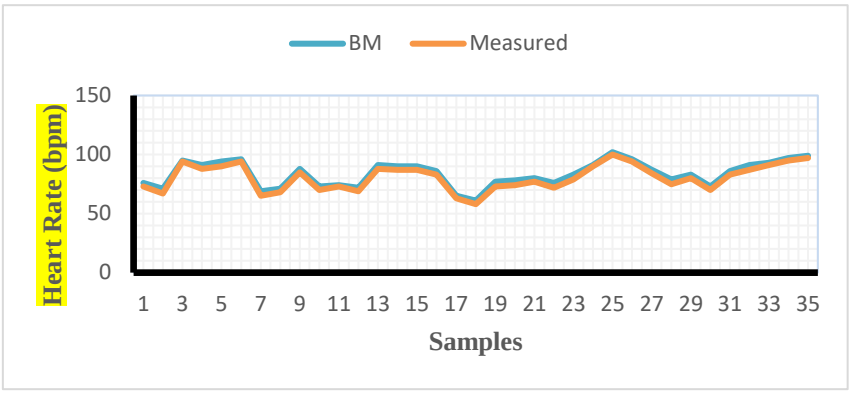

(A)

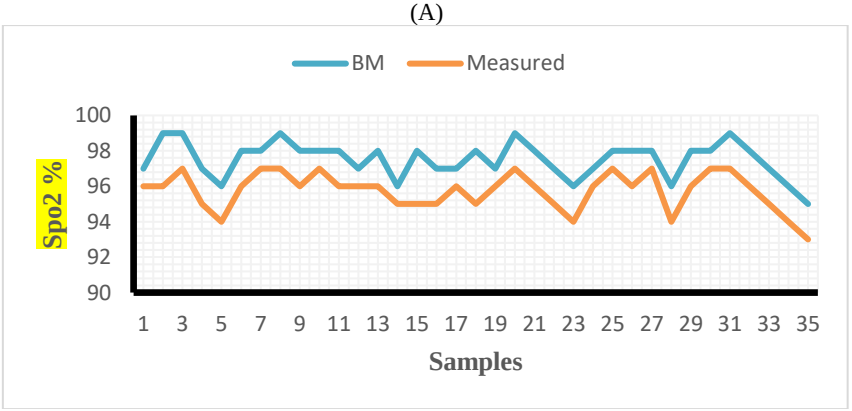

(B)

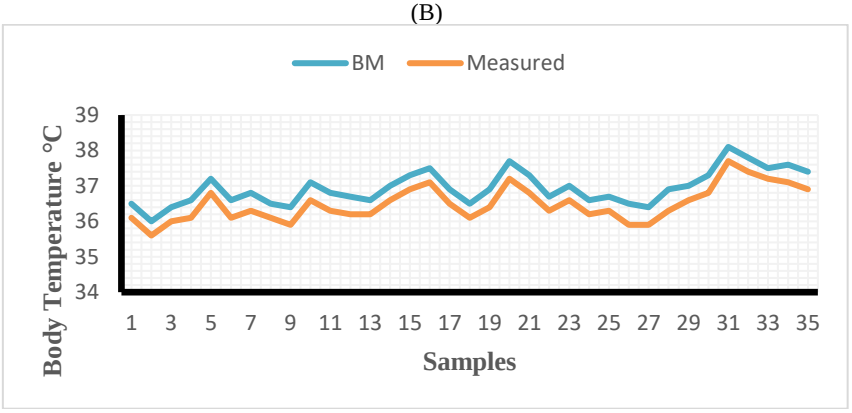

(C)

Fig. 11. (A)Heart rate, (B)Spo2, and(C) temperature readings for the healthcare station and Benchmark device (BM)

3.1.1. The test of error

For the 35 samples—35 samples each for heart rate, SpO2, and temperature—an error test and an analysis were performed. Equation (4,8) was used to determine the MAE and RMSE between the healthcare station and the BM. The MAE was determined using the absolute error estimates for every heart rate, SpO2, and temperature, shown in Figure 12 (A, B, and C). Fig. 12A demonstrates that the heart rate's absolute inaccuracy ranged from 1 to 4, while its MAE was 2.88. The absolute error of Oxygen saturation was in the range of 1 to 3 with only an MAE of 1.77, and the absolute error of temperature was also in the range of 0.3 to 0.6 with an MAE of 0.44, as shown in Figures 12B and C, respectively. That demonstrates that, when the total mistakes are given the same weight, there is a tiny inaccuracy between both the healthcare station as well as the Benchmark device BM.

$$E_i = X_i - Y_i \quad (4)$$

$$MAE = \frac{\sum |E_i|}{N} \quad (5)$$

Where E_i is the absolute error N stands for the number of samples, Xi for the estimated value, and Yi for the actual value

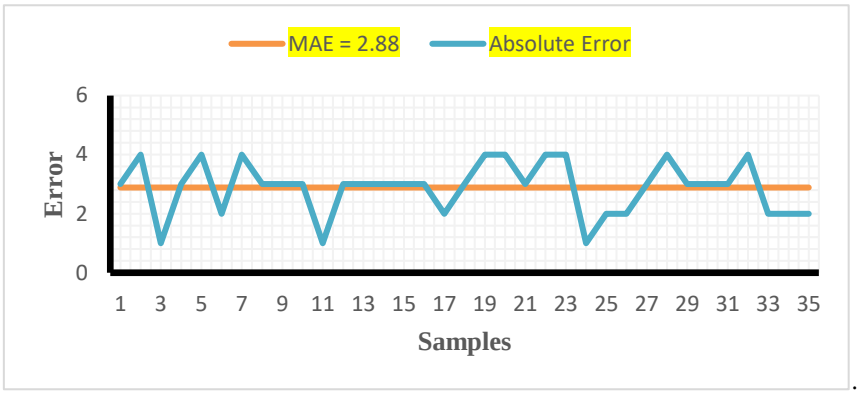

(A)

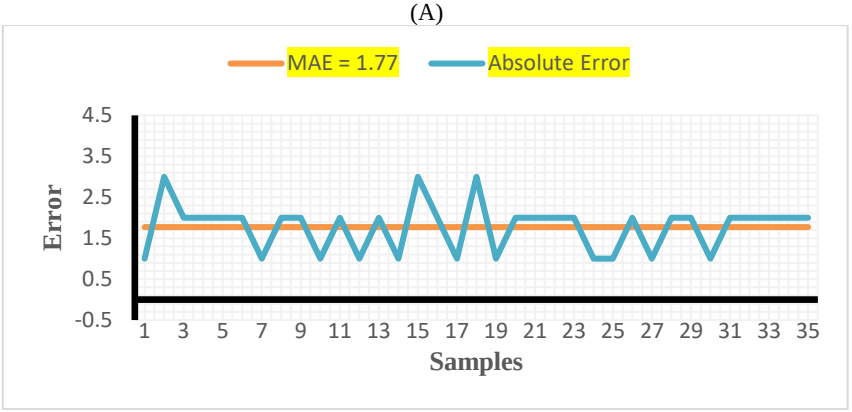

(B)

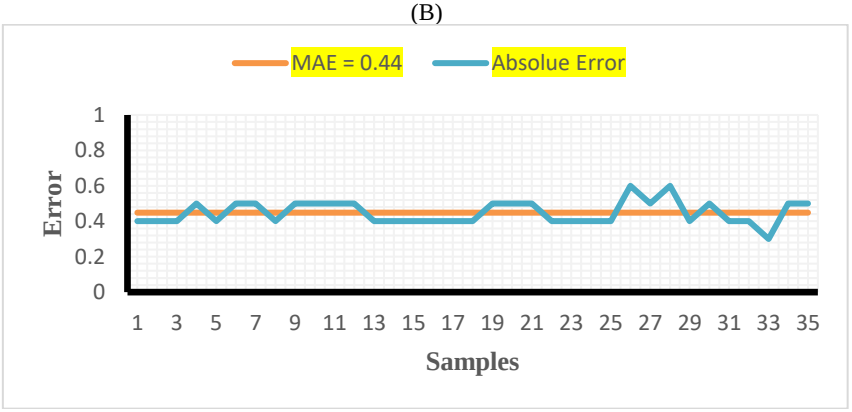

(C)

Fig. 12. The mean absolute error and the absolute error (A) Heart rate, (B) Spo2, and (C) Temperature between the healthcare station and the Benchmark device (BM)

MAPE displays an error but does not display how it relates to the real value. To demonstrate the relative inaccuracy between the healthcare station and the Benchmark device (BM) for the heart rate, Spo2, and temperature, the MAPE was computed and the results are displayed in Figs. 13 (A, B, and C). Fig. 13A displays the absolute percentage error and the MAPE of heart rate with a MAPE of 3.55 percent and a range of 1.09 percent to 5.63 percent. The absolute percentage error and the MAPE of the Spo2 are shown in Figure 13 B, with a maximum error of 3.06 percent and the lowest error of 1.02 percent, respectively. However, the actual MAPE of the Spo2 was 1.81 percent. Figure 13C displays the absolute percentage error and the MAPE of temperature in the 0.8 to 1.64 percent range, with the MAPE being 1.21 percent. The MAPE calculations indicate that the proposed healthcare station's relative error is low, which suggests that the important data readings from the proposed healthcare station are of very high quality.

$$MAPE = \frac{\sum \frac{|E_i|}{y_i}}{N} \times 100\% \quad (6)$$

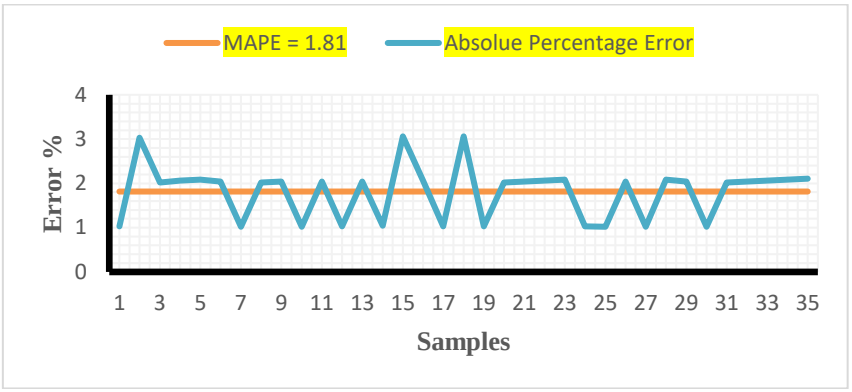

(A)

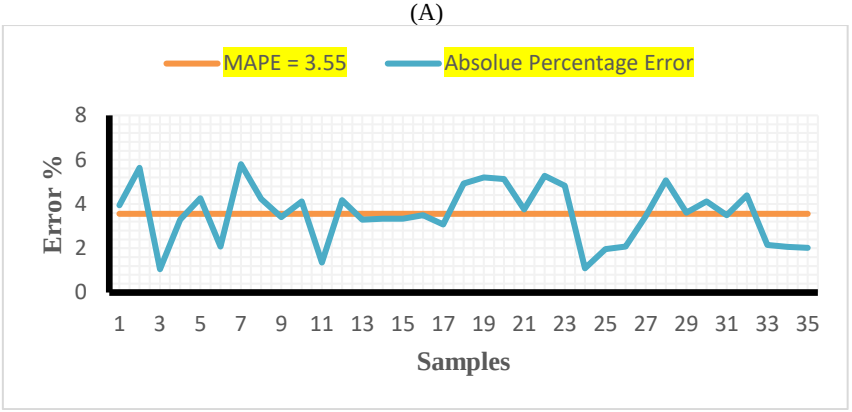

(B)

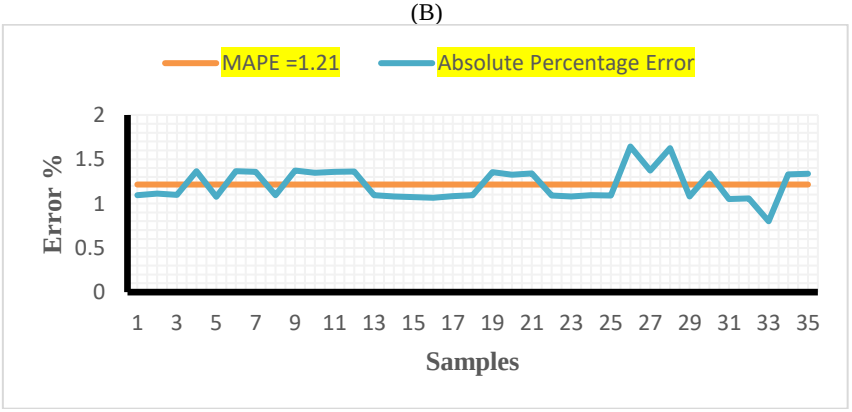

(C)

Fig. 13. The mean absolute percentage error and absolute percentage error of (A) Heart rate, (B) Spo2, and (C) Temperature between the healthcare station and the benchmark device (BM)

The MAE calculates the errors as the same weight, as was previously explained; this technique of computation regrades the outliers. The RMSE should be calculated to account for these outliers, where the RMSE gives the huge mistakes more weight to offer them a wider field of view and lessens the weight of the tiny errors. This allows for the system to be evaluated to see whether or not it regularly returns a significant error. Fig. 14A depicts the heart rate's absolute error and root mean square error (RMSE), where the RMSE was 3.01. The absolute error and RMSE of the Spo2 are shown in Fig. 14B, where the RMSE was 1.86. The absolute error and RMSE for the temperature where the RMSE is 0.45 are displayed in Fig. 14 C.

$$\mathrm{MSE} = \frac{\sum(\mathrm{E_i})^2}{\mathrm{N}} \tag{7}$$

$$\mathrm{RMSE} = \sqrt{\mathrm{MSE}} \tag{8}$$

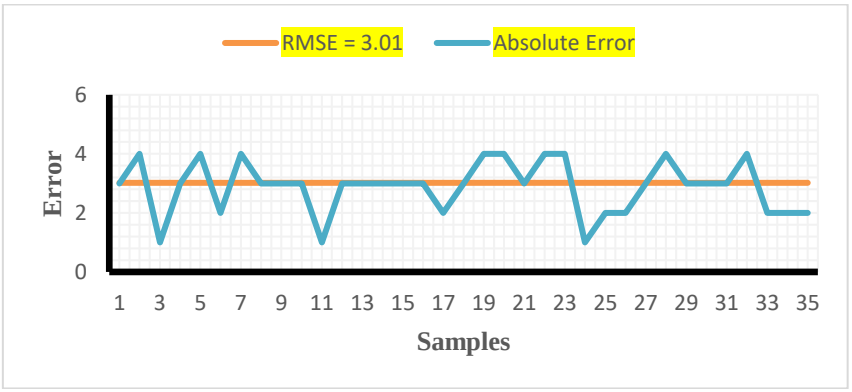

(A)

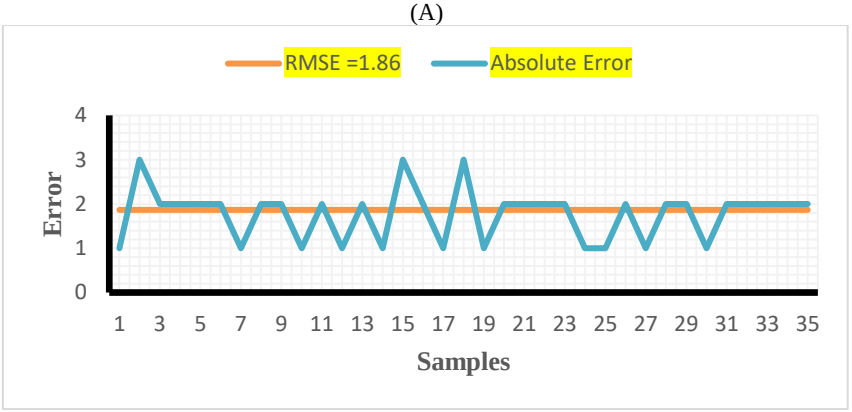

(B)

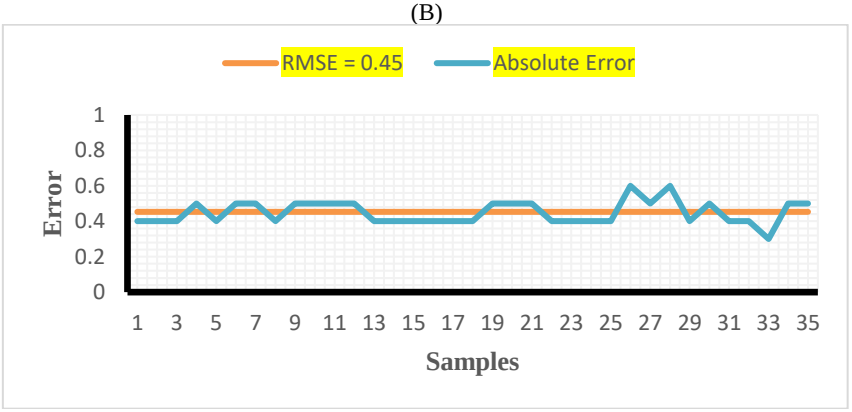

(C)

Fig. 14. The Root mean square error and Absolute error for (A) Heart rate, (B) Spo2, and (C) temperature between the healthcare station and the benchmark device (BM)

Together, the MAE and the RMSE can provide insight into the real nature of the error. When these two parameters' values are equal, the system has a constant error; nevertheless, when there is a significant discrepancy between both the MAE and the RMSE, the system produces a wide range of errors. The system is unstable as a result. The system has a tiny variance in the errors that are deemed acceptable if there is a slight discrepancy between both the MAE and the RMSE.

Fig. 15 A displays the heart rate's MAE, RMSE, and absolute error. It reveals that the MAE is 2.88 and the RMSE is 3.01. The identical values for the Spo2 are shown in Fig. 15 B with an MAE of 1.77 and an RMSE of 1.86. Additionally, Fig. 15 C displays these temperature-related metrics with RMSE and MAE of 0.45 and 0.44, respectively. This indicates that its outliers in the healthcare station are non-recurring as well as the system has a tiny and consistent error, making the healthcare station and BM nearly identical. These results also reveal very little difference between the MAE and the RMSE.

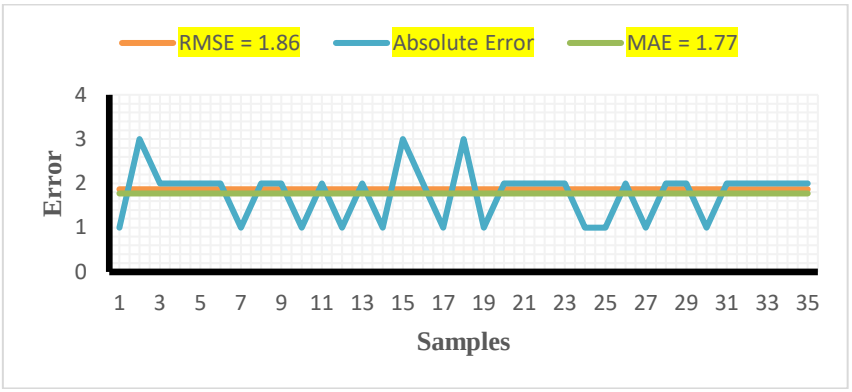

(A)

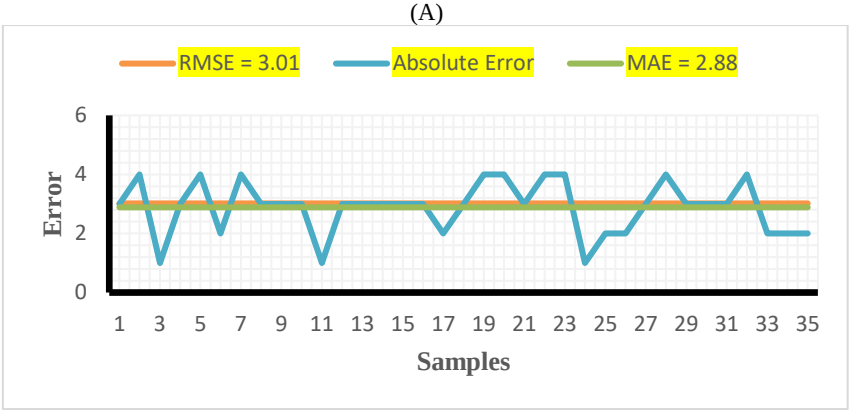

(B)

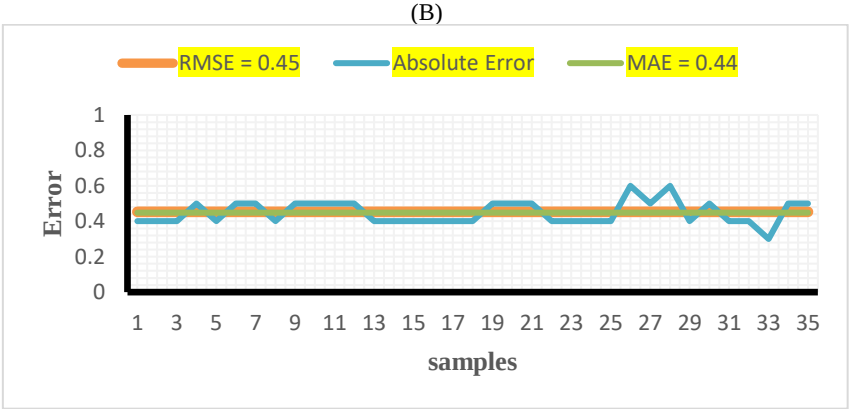

(C)

Fig. 15. The MAE, RMSE, and Absolute error for (A) Heart rate, (B) Spo2, and (C) temperature

3.1.2. Pearson Correlation Coefficient (r)

Pearson Correlation is a descriptive statistical method that was used to compare the Actual value and the Measured value of each vital sign of the Healthcare station to see if there were a linear relationship between the two quantitative variables or not according to Equation (9). Figures 16 A, B and C show the relationship between the two quantitative variables. The value of (r) for heart rate was 0.99 and 0.835 for Spo2 and 0.99 for temperature which means that there is a positive correlation. The behavior of the BM same as the healthcare station.

$$r = \frac{\sum(X-\bar{X})(Y-\bar{Y})}{\sqrt{\sum(X-\bar{X})^2}\sqrt{(Y-\bar{Y})^2}} \quad (9)$$

Where X is the measured Values and $\bar{X}$ is the Mean of measured values, Y is the actual value and $\bar{Y}$ is the mean of actual values X - $\bar{X}$ & Y - $\bar{Y}$ is the Deviation scores.

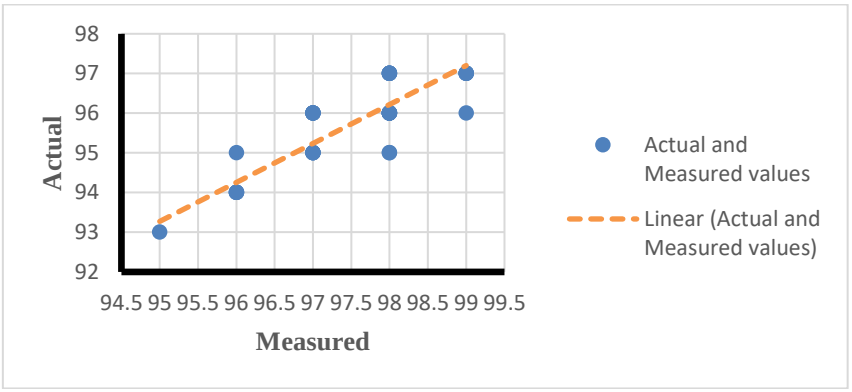

(A)

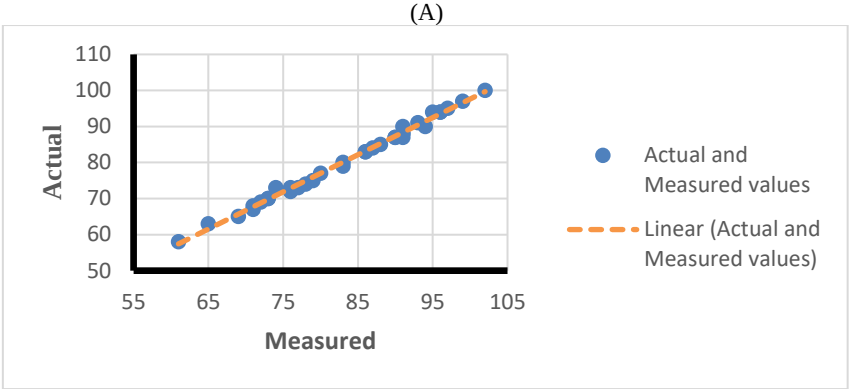

(B)

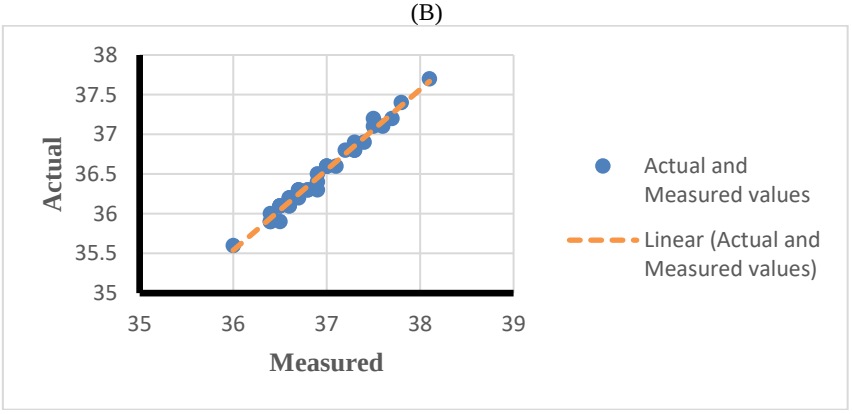

(C)

Fig. 16. The Pearson Correlation Coefficient for (A) Heart rate, (B) Spo2, and (C) temperature

3.2. Current Consumptions Calculations

In this section, the power consumption will be calculated by using the multimeter of type (ASWAR AS-M108B), and battery capacity calculated according to Equation (10). The current consumption was calculated, as shown in Table 2.

$$\text{Battery life} = \frac{\text{I battery capacity}}{\text{I}_{\text{avarege Station}}} \quad (10)$$

Table 2. Current consumption for healthcare station

Stations	I average mA	Battery mA/H	Estimated battery life/Hour
Healthcare Station	137	1200	8.75

3.3. Comparison between healthcare station and related works

A comparison between the proposed system and other related works was made according to different parameters. These parameters are device accuracy and current consumption.

3.3.1. The Accuracy Comparison

The accuracy of the healthcare station was compared to that of comparable works[22–26] Heartrate, Spo2, and temperature accuracy of 96.54 %, 98.18 %, and 98.78 %, respectively, in this comparison demonstrated the system's superiority, depending on Equation (11).

$$\text{Accuracy} = \left(1 - \frac{\left|\frac{\sum_i^n \text{EST}_i}{n} - \frac{\sum_i^n \text{Actual}_i}{n}\right|}{\frac{\sum_i^n \text{Actual}_i}{n}}\right) \times 100\% \quad (11)$$

The accuracy was 97.63 % overall when these three parameters were averaged. The contrast between the healthcare station and other systems is seen in Fig. 17.

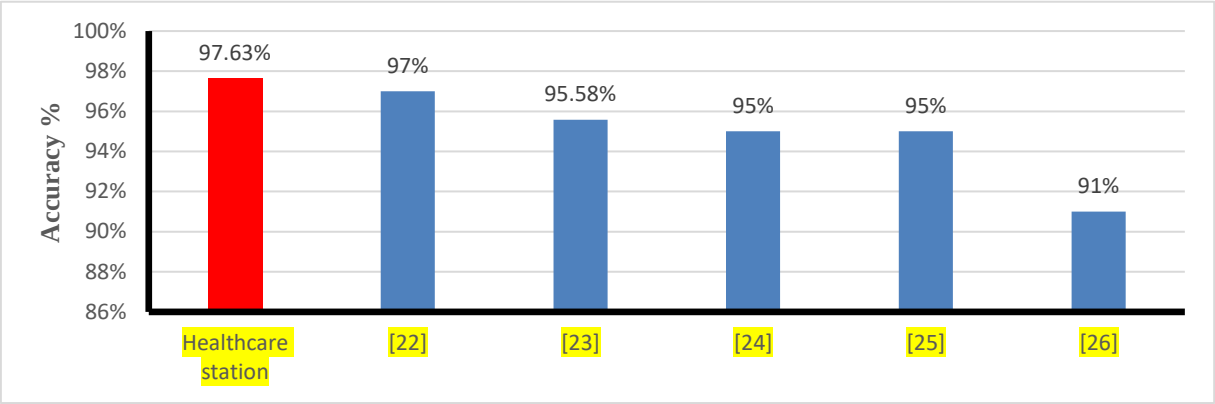

Fig. 17. Accuracy comparison between healthcare station and related works

3.3.2. Current Consumption Comparison

When comparing the healthcare station with the related works[27–31], the healthcare station consumes an appropriate current, considering the benefits that it gives. The current consumption can even be reduced further. However, this reduction will negatively affect the objectives of this thesis. Fig. 18 shows the comparison between healthcare stations and related works in terms of current consumption.

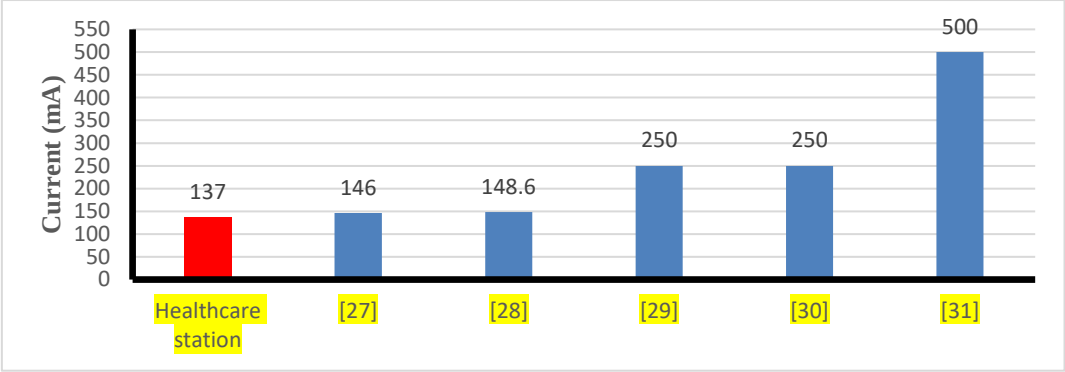

Fig. 18. Current consumption comparison between healthcare stations and related works

3.4. Comparison of LoRa Performance

The healthcare station and accompanying works were contrasted. [32–35] in terms of the distance that LoRa can go outside of the workplace. This comparison demonstrated the system's advantage at a distance of 1,400 meters. The contrast between the healthcare station and other systems is seen in Fig. 19.

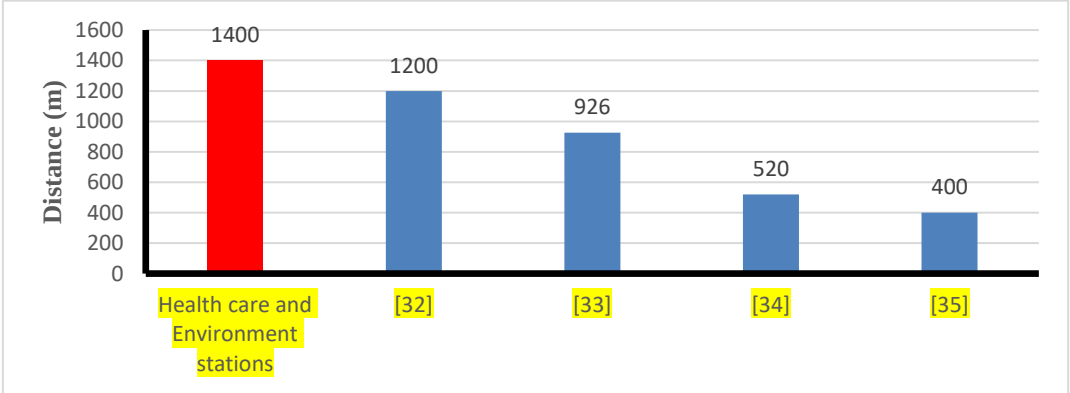

Fig. 19. LoRa performance comparison between the healthcare station and other systems

4. Conclusions

This research has successfully designed and implemented a healthcare station for measuring pulse rate, oxygen saturation, and body temperature for patients and workers in maintenance using the MAX30100 sensor and tMLX90614 sensor. The MAX30100 sensor can be utilized to measure the heart rate and Spo2 while the MLX90614 sensor can be used to measure body temperature with IR features that enable it to use the station for Covid-19 patients that avoid direct contact with the body, to prevent the spread of Covid-19. The ESP32 Node's measurement data were transferred to a monitoring station using LoRa which provides indoor and outdoor work for the system. The instrument's accuracy was 97.63 %. If the abnormalities in the recorded parameters are detected, then an alert will be triggered (buzzer and blinking LED) Thus, the instrument is functioning well and is suitable for use.

Acknowledgment

we would like to thank the staff of Al-Imam Al-Sadiq Hospital, especially the maintenance staff who provided me with support and assistance in accomplishing this work by providing the necessary equipment to compare it with our device.

Reference

[1] S. Chandra Mukhopadhyay, “Wearable Sensors for Human Activity Monitoring,” IEEE Sensors Journal, vol. 15, no. 3. pp. 1321–1330, 2015.
[2] B. Sundara, K. C. Sarvepalli, and S. H. Davuluri, “GSM Based patient monitoring system in NICU,” IJRET Int. J. Res. Eng. Technol., vol. 2, no. 07, 2013.
[3] S. Majumder, T. Mondal, and M. J. Deen, “Wearable sensors for remote health monitoring,” Sensors (Switzerland), vol. 17, no. 1. 2017, doi: 10.3390/s17010130.
[4] D. Dias and J. P. S. Cunha, “Wearable health devices—vital sign monitoring, systems and technologies,” Sensors (Switzerland), vol. 18, no. 8. 2018, doi: 10.3390/s18082414.
[5] C. Rotariu, H. Costin, G. Andruseac, R. Ciobotariu, and F. Adochiei, “An integrated system for wireless monitoring of chronic patients and elderly people,” in 15th International Conference on System Theory, Control and Computing, 2011, pp. 1–4.
[6] T. Tamura, Y. Maeda, M. Sekine, and M. Yoshida, “Wearable photoplethysmographic sensors—past and present,” Electronics, vol. 3, no. 2, pp. 282–302, 2014.
[7] R. Sameh, M. Genedy, A. Abdeldayem, and M. H. Abdel Azeem, “Design and Implementation of an SPO2 Based Sensor for Heart Monitoring Using an Android Application,” in Journal of Physics: Conference Series, 2020, vol. 1447, no. 1, doi: 10.1088/1742-6596/1447/1/012004.
[8] C. Rotariu and V. Manta, “Wireless system for remote monitoring of oxygen saturation and heart rate,” 2012 Federated Conference on Computer Science and Information Systems, FedCSIS 2012. pp. 193–196, 2012.
[9] L. Giovangrandi, O. T. Inan, D. Banerjee, and G. T. A. Kovacs, “Preliminary results from BCG and ECG measurements in the heart failure clinic,” in 2012 Annual International Conference of the IEEE Engineering in Medicine and Biology Society, 2012, pp. 3780–3783.
[10] Mayo Clinic Staff, “Fever: First aid - Mayo Clinic,” Mayo Clinic, 2019. https://www.mayoclinic.org/first-aid/first-aid-fever/basics/art-20056685 (accessed Aug. 10, 2022).
[11] E. A. Suprayitno, M. R. Marlianto, and M. I. Mauliana, “Measurement device for detecting oxygen saturation in blood, heart rate, and temperature of human body,” in Journal of Physics: Conference Series, 2019, vol. 1402, no. 3, doi: 10.1088/1742-6596/1402/3/033110.
[12] M. J. Buller, W. J. Tharion, R. W. Hoyt, and O. C. Jenkins, “Estimation of human internal temperature from wearable physiological sensors,” 2010.
[13] E. Gaura, J. Kemp, and J. Brusey, “Leveraging knowledge from physiological data: On-body heat stress risk prediction with sensor networks,” IEEE Trans. Biomed. Circuits Syst., vol. 7, no. 6, pp. 861–870, 2013.
[14] V. R. Parihar, A. Y. Tonge, and P. D. Ganorkar, “Heartbeat and Temperature Monitoring System for Remote Patients using Arduino,” International Journal of Advanced Engineering Research and Science, vol. 4, no. 5. pp. 55–58, 2017, doi: 10.22161/ijaers.4.5.10.
[15] A. N. Costrada, A. G. Arifah, I. D. Putri, I. K. A. Sara Sawita, H. Harmadi, and M. Djamal, “Design of Heart Rate, Oxygen Saturation, and Temperature Monitoring System for Covid-19 Patient Based on Internet of Things (IoT),” J. ILMU Fis. | Univ. ANDALAS, vol. 14, no. 1, pp. 54–63, 2022, doi: 10.25077/jif.14.1.54-63.2022.
[16] M. A. Pertiwi, I. D. Gede Hari Wisana, T. Triwiyanto, and S. Sukaphat, “Measurement of Heart Rate, and Body Temperature Based on Android Platform,” Indonesian Journal of electronics, electromedical engineering, and medical informatics, vol. 2, no. 1. pp. 26–33, 2020, doi: 10.35882/ijeeemi.v2i1.6.
[17] R. K. Kodali, S. Yerroju, and B. Y. Krishna Yogi, “IoT Based Wearable Device for Workers in Industrial Scenarios,” IEEE Region 10 Annual International Conference, Proceedings/TENCON, vol. 2018-Octob. pp. 1893–1898, 2019, doi: 10.1109/TENCON.2018.8650187.
[18] Pras, “How pulse oximeters work explained simply,” 2021. https://www.howequipmentworks.com/pulse_oximeter/ (accessed Jul. 07, 2022).
[19] “WIFI LoRa 32 (V2) – Heltec Automation.” https://heltec.org/project/wifi-lora-32/ (accessed Jul. 07, 2022).
[20] “Amazon.com: MakerFocus ESP32 LoRa 32 (V2), ESP32 Development Board W I F I Bluet ooth LoRa Dual Core 240MHz CP2102 with 0.96inch OLED Display Included 868/915MHZ Antenna for Smart Cities, Smart Farms, Smart Home : Electronics.” https://www.amazon.com/MakerFocus-Development-Bluetooth-0-96inch-Display/dp/B076MSLFC9 (accessed Aug. 10, 2022).
[21] “B40 Patient Monitor | Patient Monitoring | GE Healthcare (United Kingdom).” https://www.gehealthcare.co.uk/products/patient-monitoring/patient-monitors/b40-patient-monitor (accessed Aug. 10, 2022).
[22] M. S. Islam, M. T. Islam, A. F. Almutairi, G. K. Beng, N. Misran, and N. Amin, “Monitoring of the human body signal through the Internet of Things (IoT) based LoRa wireless network system,” Appl. Sci., vol. 9, no. 9, 2019, doi: 10.3390/app9091884.
[23] M. M. Ali, S. Haxha, M. M. Alam, C. Nwibor, and M. Sakel, "Design of Internet of Things (IoT) and Android Based Low Cost Health Monitoring Embedded System Wearable Sensor for Measuring SpO2, Heart Rate, and Body Temperature Simultaneously," Wirel. Pers. Commun., vol. 111, no. 4, pp. 2449–2463, 2020, doi: 10.1007/s11277-019-06995-7.

[24] U. Gogate and J. Bakal, "Healthcare monitoring system based on wireless sensor network for cardiac patients," Biomedical and Pharmacology Journal, vol. 11, no. 3. pp. 1681–1688, 2018, doi: 10.13005/bpj/1537.
[25] M. M. Islam, A. Rahaman, and M. R. Islam, "Development of Smart Healthcare Monitoring System in IoT Environment," SN Comput. Sci., vol. 1, no. 3, pp. 1–11, 2020, doi: 10.1007/s42979-020-00195-y.
[26] M. Nosrati and N. Tavassolian, "High-Accuracy Heart Rate Variability Monitoring Using Doppler Radar Based on Gaussian Pulse Train Modeling and FTPR Algorithm," IEEE Trans. Microw. Theory Tech., vol. 66, no. 1, pp. 556–567, 2018, doi: 10.1109/TMTT.2017.2721407.
[27] A. Ngu, Y. Wu, H. Zare, A. Polican, B. Yarbrough, and L. Yao, "Fall detection using smartwatch sensor data with accessor architecture," Lect. Notes Comput. Sci. (including Subser. Lect. Notes Artif. Intell. Lect. Notes Bioinformatics), vol. 10347 LNCS, pp. 81–93, 2017, doi: 10.1007/978-3-319-67964-8_8.
[28] A. Mdhaffar, T. Chaari, K. Larbi, M. Jmaiel, and B. Freisleben, "IoT-based health monitoring via LoRaWAN," 17th IEEE Int. Conf. Smart Technol. EUROCON 2017 - Conf. Proc., no. July, pp. 519–524, 2017, doi: 10.1109/EUROCON.2017.8011165.
[29] U. Ijaz, U. Ameer, H. Tarar, A. Ilyas, and A. Ijaz, "E-health acquistion, transmission & monitoring system," Proc. 2017 2nd Work. Recent Trends Telecommun. Res. RTTR 2017, pp. 0–3, 2017, doi: 10.1109/RTTR.2017.7887868.
[30] R. Prakash, A. B. Ganesh, and S. V. Girish, "Cooperative wireless network control based health and activity monitoring system," J. Med. Syst., vol. 40, no. 10, 2016, doi: 10.1007/s10916-016-0576-4.
[31] G. López, V. Custodio, and J. I. Moreno, "LOBIN: E-textile and wireless-sensor-network-based platform for healthcare monitoring in future hospital environments," IEEE Trans. Inf. Technol. Biomed., vol. 14, no. 6, pp. 1446–1458, 2010, doi: 10.1109/TITB.2010.2058812.
[32] G. B. Tayeh, J. Azar, A. Makhoul, C. Guyeux, and J. Demerjian, "A Wearable LoRa-Based Emergency System for Remote Safety Monitoring," 2020 Int. Wirel. Commun. Mob. Comput. IWCMC 2020, pp. 120–125, 2020, doi: 10.1109/IWCMC48107.2020.9148359.
[33] F. Wu, T. Wu, and M. R. Yuce, "An internet-of-things (IoT) network system for connected safety and health monitoring applications," Sensors (Switzerland), vol. 19, no. 1, 2019, doi: 10.3390/s19010021.
[34] F. Wu, J. M. Redoute, and M. R. Yuce, "WE-safe: A self-powered wearable IoT sensor network for safety applications based on lora," IEEE Access, vol. 6, pp. 40846–40853, 2018, doi: 10.1109/ACCESS.2018.2859383.
[35] F. Wu, C. Qiu, T. Wu, and M. R. Yuce, "Edge-Based Hybrid System Implementation for Long-Range Safety and Healthcare IoT Applications," IEEE Internet Things J., vol. 8, no. 12, pp. 9970–9980, 2021, doi: 10.1109/JIOT.2021.3050445.